and several other laminar shear stress-upregulated genes were identified in the subtracted library, as noted above.

3.6. Some RECS genes are upregulated in aortic atherosclerotic lesions

As a first step towards investigating the relevance of the *RECS* genes to atherosclerosis, we analyzed their expression in atherosclerotic tissues from a human aorta by Northern blotting. Among the 13 genes examined, four genes, *RECS10*, *-12*, *-26* and *-32*, show elevated levels of mRNA in atherosclerotic lesions as compared with normal regions of the aorta (Fig. 5). Since these genes are unknown or are of unknown function, they may be novel candidate genes for atherogenesis. On the other hand, four genes, *RECS42*, *-46*, *-58* and *-63*, do not show any differences in patterns of expression (data not shown). Furthermore, clear bands could not be detected for five genes, *RECS16*, *-28*, *-41*, *-44* and *-49* (data not shown), suggesting that the expression of these genes may be relatively low or may be specific to endothelial cells, which constitute a minor population of aortic cells.

4. Discussion

Several techniques for differential cloning have been developed, such as differential display, subtraction, differential hybridization and DNA microarray analysis. Differential display has been the most commonly used method over the past decade, and some groups have reported the identification of shear stress-responsive genes using this procedure [3,7,27]. However, a strong bias towards abundant mRNAs is a potential disadvantage of differential display [28]. Although DNA microarrays are very powerful tools, available arrays do not have a complete set of human genes, which makes the development of efficient methods for differential cloning still necessary. In this study, we used subtraction and reverse subtraction methods that we devised to obtain a number of genes, termed *RECS*, whose expression in HUVEC is upregulated by non-uniform flow. It should be noted that only 13 out of 63 genes were represented more than once-namely, there were 50 unique genes among 82 total clones that were represented only once and only 19 replicates were extra copies of those 13 genes (Table 2). The result indicates that the subtracted library is normalized, as was the case for our previous subtraction [12].

Among the identified genes, several are already known to be upregulated by laminar shear stress, such as MCP-1, HB-EGF, laminin B1, TM, TGF-β and thrombospondin. Since we used a turbulent shear stress apparatus, these genes are unlikely to be laminar shear stress-specific, which is supported by reports showing that TM is upregulated by both laminar and turbulent shear stress [4,10]. An inverse observation is that four of five *RECS* genes tested are also upregulated by exposure to laminar shear stress in a parallel plate chamber (Fig. 4).

We also found genes with homology to known genes or sequences, but of unknown function. *RECS1* is significantly homologous to rat NMP35 (51% identity), which is specifically expressed in the central nervous system, but whose function has not yet been determined [24]. *RECS12* is the cytokine-response gene CR8, which encodes a basic helix-loop-helix transcription factor [29] that is expressed in human embryo chondrocytes treated with Bt2cAMP. *RECS26*, which is an anonymous gene named KIAA0025, was encountered three times during our Northern screening. Its deduced amino acid sequence does not show any significant similarity to known proteins. Recently, however, KIAA0025 has been reported to be strongly activated by treatment of human skin fibroblast with the alkylating agent methylmethanesulfonate or by osmotic shock [30], and to have a functional endoplasmic reticulum stress-responsive element in its 5′ flanking region, which may also be related to shear stress-responsiveness. *RECS10* has been identified only as an EST and has no distinct open reading frame. Although their biological functions are still unknown, these genes possibly have some relevance to atherosclerosis, like the known lami-

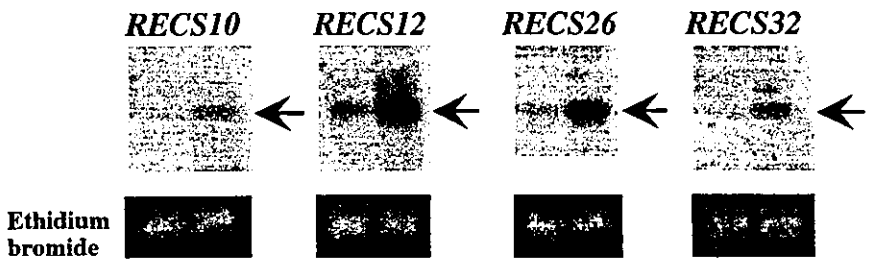

Fig. 5. Expression of selected *RECS* genes in human aorta. Four micrograms of total RNA from atherosclerotic lesions and from normal regions of human aorta were loaded in the right and left lanes, respectively, of each gel, followed by Northern hybridization analysis. A specific band in each blot is indicated by an arrow. Ethidium bromide staining of 28 S ribosomal RNA before blotting serves as a loading control.

nar flow-upregulated genes noted above. However, it is difficult to infer from their laminar flow-upregulation that they are antiatherogenic factors, because they are also upregulated by non-laminar flow, as in the case of MCP-1, HB-EGF and thrombospondin, all of which are known to be atherogenic.

In contrast, representative atheroprotective genes such as ecNOS, COX-2 and Mn-SOD are reported to be specifically upregulated by laminar shear stress [7]. It should be noted that some genes in Table 2 are or can be considered atheroprotective but have not been shown to be responsive to shear stress. Deficient or decreased enzymatic activity of lysosomal acid lipase (*RECS43*) has previously been reported to cause cholesterol ester storage disease, which in most cases is associated with premature atherosclerosis and low plasma HDL cholesterol [31]. N^G,N^G-dimethylarginine dimethylaminohydrolase (DDAH; *RECS44*) hydrolyzes asymmetric dimethylarginine (ADMA), which is an endogenous competitive inhibitor of NOS and whose plasma levels are elevated in patients with hypercholesterolemia or atherosclerosis. It has been shown that DDAH activity, but not its expression level, is disrupted in human endothelial cells stimulated with oxidized LDL (oxLDL) or TNF-β and that the concentration of ADMA is accordingly increased in the conditioned medium [32]. Laminar flow-dependent expression patterns for these two putative atheroprotective genes remain to be examined.

On the other hand, the levels of ET-1 and PAI mRNA, neither of which had previously been found to be upregulated by laminar flow [9,22,23], were shown in this study to be dramatically increased, in striking contrast to the genes noted above which are upregulated by both laminar and non-laminar flow. This clearly suggests that these representative proatherogenic genes, for which an elevated expression is observed in human atherosclerotic lesions [33,34], are upregulated by non-uniform flow but are downregulated or unchanged by laminar flow. *RECS7*, which is probably a novel GAP because of its significant homology to known GAPs, such as the SH3 domain binding protein [26], is not upregulated by laminar shear stress (data not shown), suggesting that this novel GAP may function as an atherogenic signaling molecule. Also found were several genes that are known to be atherogenic but whose responsiveness to fluid flow has not been reported. IL-8 has recently been shown to recruit monocytes to the endothelium [35] and has previously been reported not only in atherosclerotic plaques but also in circulating macrophages from patients with atherosclerosis [36]. Although macrophages are a major source of IL-8 in atherosclerotic lesions, endothelial cells also express IL-8 in vitro in response to atherogenic stimuli, such as oxLDL [37]. CTGF is also reported to be expressed at higher levels in advanced atherosclerotic lesions of carotid arteries than in non-atherosclerotic arteries [38]. It has recently been demonstrated that CTGF induces apoptosis in human smooth muscle cells [39], but the importance of CTGF in atherogenesis has yet to be clarified. Cyr61 (*RECS32*), an immediate-early gene that belongs to the CTGF family, has recently been identified as a potent angiogenic inducer that enhances the tumorigenicity of tumor cells [40], but its relevance to atherogenesis is not known (see below). Matrix Gla protein (*RECS52*), an extracellular matrix protein, is shown here to be highly expressed in human atherosclerotic plaques, and its expression is closely associated with vascular calcification [41].

Lastly, we have demonstrated that the mRNAs of four *RECS* genes are expressed at higher levels in atherosclerotic lesions of the human aorta than in normal regions (Fig. 5). Three of the four (*RECS10*, *-12* and *-26*) are genes whose functions remain unclear, but whose in vitro expression in endothelial cells has been shown in this study to be upregulated not only by non-uniform but also by laminar flow; and the fourth (*RECS32*) is Cyr61, which has a known angiogenic function (noted above). Like known atherogenic genes whose high expression in atherosclerotic lesions has been reported, these four *RECS* genes may play an important role in the initiation or progression of atherosclerosis. That the nine other *RECS* genes examined are either unexpressed or exhibit a constant level of expression, does not exclude the possibility that they have an atherogenic function. Precise expression analysis by immunohistochemistry and functional validation using full-length cDNAs would clarify the relevance of these genes to atherosclerosis. Given that we have found several known atherosclerosis-related genes and some candidate atherogenic genes in the subtracted library, at least some *RECS* genes might be involved in the pathogenesis of atherosclerosis, in which they are more likely be atherogenic than atheroprotective. Functional analyses of the *RECS* genes that were previously unidentified or of unknown function, or those previously regarded as unrelated to atherosclerosis are underway in our laboratory.

Acknowledgements

We thank Dr Kazutoshi Tamura for support in the construction of the cDNA library. We are grateful to Reiko Kohda and Hiromi Inagaki for their help in DNA sequencing. We also thank Dr Satoshi Nakagawa, Hironori Kawai and Naoko Tateishi for their bioinformatics work. This work was supported by grants from the Ministry of Education, Science and Culture, Japan and ONO Medical Research Foundation.

References

[1] Ross R. Atherosclerosis—an inflammatory disease. New Engl J Med 1999;340:115–26.

[2] Nerem RM. Vascular fluid mechanics, the arterial wall, and atherosclerosis. J Biomech Eng 1992;114:274–82.

[3] Topper JN, Gimbrone MA Jr. Blood flow and vascular gene expression: fluid shear stress as a modulator of endothelial phenotype. Mol Med Today 1999;5:40–6.

[4] Resnick N, Yahav H, Schubert S, Wolfovitz E, Shay A. Signalling pathways in vascular endothelium activated by shear stress: relevance to atherosclerosis. Curr Opin Lipidol 2000;11:167–77.

[5] Traub O, Berk BC. Laminar shear stress: mechanism by which endothelial cells transduce an atheroprotective force. Arterioscler Thromb Vasc Biol 1998;81:677–85.

[6] Corson MA, James NL, Latta SE, Neren RM, Berk BC, Harrison DG. Phosphorylation of endothelial nitric oxide synthase in response to fluid shear stress. Circ Res 1996;79:984–91.

[7] Topper JN, Cai J, Falb D, Gimbrone MA Jr. Identification of vascular endothelial genes differentially responsive to fluid mechanical stimuli: COX-2, MnSOD and ecNOS are selectively upregulated by steady laminar shear stress. Proc Natl Acad Sci USA 1996;93:10417–22.

[8] Ando J, Tsuboi H, Korenaga R, Takada Y, Toyama-Sorimachi N, Miyasaka M, Kamiya A. Shear stress inhibits adhesion of cultured mouse endothelial cells to lymphocytes by downregulating VCAM-1 expression. Am J Pathol 1994;267:C679–87.

[9] Sharefkin JB, Diamond SL, Eskin SG, McIntire LV, Dieffenbach CW. Fluid flow decreases preproendothelin mRNA levels and suppresses endothelin-1 peptide release in cultured human endothelial cells. J Vasc Surg 1991;14:1–9.

[10] Takada Y, Shinkai F, Kondo S, Yamamoto S, Tsuboi H, Korenaga R, Ando J. Fluid shear stress increases the expression of thrombomodulin by cultured human endothelial cells. Biochem Biophys Res Commun 1994;205:1345–52.

[11] Malek AM, Jackman R, Rosenberg RD, Izumo S. Endothelial expression of thrombomodulin is reversibly regulated by fluid shear stress. Circ Res 1994;74:852–60.

[12] Kobori M, Ikeda Y, Nara H, Kato M, Kumegawa M, Nojima H, Kawashima H. Large scale isolation of osteoclast-specific genes by an improved method involving the preparation of a subtracted cDNA library. Genes Cells 1998;3:459–75.

[13] Cooke JP, Stamler J, Andon N, Davies PF, Mckinley G, Loscalzo J. Flow stimulates endothelial cells to release a nitrovasodilator that is potentiated by reduced thiol. Am J Physiol 1990;259:H804–12.

[14] Taba Y, Sasaguri T, Miyagi M, Abumiya T, Miwa Y, Ikeda T, Mitsumata M. Fluid shear stress induces lipocalin-type prostaglandin D_2 synthase expression in vascular endothelial cells. Circ Res 2000;86:967–73.

[15] Diamond SL, Sharefkin JB, Dieffenbach C, Frasier-Scott K, McIntire LV, Eskin SG. Tissue plasminogen activator messenger RNA levels increase in cultured human endothelial cells exposed to laminar shear stress. J Cell Physiol 1990;143:364–71.

[16] Hsieh H-J, Li N-Q, Frangos JA. Shear stress increases endothelial platelet-derived growth factor mRNA levels. Am J Physiol 1991:260:H642–6.

[17] Chun T-H, Itoh H, Ogawa Y, et al. Shear stress augments expression of C-type natriuretic peptide and adrenomedullin. Hypertension 1997;29:1296–302.

[18] Shyy Y-J, Hsieh H-J, Usami S, Chien S. Fluid shear stress induces a biphasic response of human monocyte chemotactic protein 1 gene expression in vascular endothelium. Proc Natl Acad Sci USA 1994;91:4678–82.

[19] Morita T, Yoshizumi M, Kurihara H, Maemura K, Nagai R, Yazaki Y. Shear stress increases heparin-binding epidermal growth factor-like growth factor mRNA levels in human vascular endothelial cells. Biochem Biophys Res Commun 1993;197:256–62.

[20] Throumine O, Nerem RM, Girard PR. Changes in organization and composition of the extracellular matrix underlying cultured endothelial cells exposed to laminar steady shear stress. Lab Invest 1995;73:565–76.

[21] Ohno M, Cooke JP, Dzau VJ, Gibbons GH. Fluid shear stress induces endothelial transforming growth factor beta-1 transcription and production. Modulation by potassium channel blockade. J Clin Invest 1995;95:1363–9.

[22] Kawai Y, Matsumoto Y, Watanabe K, et al. Hemodynamic forces modulate the effects of cytokines on fibrinolytic activity of endothelial cells. Blood 1996;87:2314–21.

[23] Diamond SL, Eskin SG, McIntire LV. Fluid flow stimulates tissue plasminogen activator secretion by cultured human endothelial cells. Science 1989;243:1483–5.

[24] Schweitzer B, Taylor V, Welcher AA, McClelland M, Suter U. Neural membrane protein 35 (NMP35): a novel member of a gene family which is highly expressed in the adult nervous system. Mol Cell Neurosci 1998;11:260–73.

[25] Bergelson JM, Cunningham JA, Droguett G, et al. Isolation of a common receptor for coxsackie B viruses and adenoviruses 2 and 5. Science 1997;275:1320–3.

[26] Homma Y, Emori Y. A dual functional signal mediator showing RhoGAP and phospholipase C-delta stimulating activities. EMBO J 1995;14:286–91.

[27] Ando J, Tsuboi H, Korenaga R, et al. Differential display and cloning of shear stress-responsive messenger RNAs in human endothelial cells. Biochem Biophys Res Commun 1996;225:347–51.

[28] Bertioli DJ, Schlichter UHA, Adams MJ, Burrows PR, Steinbib H-H, Antoniw JF. An analysis of differential display shows a strong bias towards high copy number mRNAs. Nucleic Acids Res 1995;23:4520–3.

[29] Shen M, Kawamoto T, Yan W, et al. Molecular characterization of the novel basic helix-loop-helix protein DEC1 expressed in differentiated human embryo chondrocytes. Biochem Biophys Res Commun 1997;236:294–8.

[30] Laar T, Schouten T, Hoogervorst E, Eck M, Eb AJ, Terleth C. The novel MMS-inducible gene Mif/KIAA0025 is a target of the unfolded protein response pathway. FEBS Lett 2000;469:123–31.

[31] Seedorf U, Wiebusch H, Muntoni S, et al. A novel variant of lysosomal acid lipase ($Leu_{336} \rightarrow Pro$) associated with acid lipase deficiency and cholesterol ester storage disease. Arterioscler Thromb Vasc Biol 1995;15:773–8.

[32] Ito A, Tsao PS, Adimoolam S, Kimoto M, Ogawa T, Cooke JP. Novel mechanism for endothelial dysfunction: dysregulation of dimethylarginine dimethylaminohydrolase. Circulation 1999;99:3092–5.

[33] Jones GT, Rij AM, Solomon C, Thomson IA, Packer SGK. Endothelin-1 is increased overlying atherosclerotic plaques in human arteries. Atherosclerosis 1996;124:25–35.

[34] Schneiderman J, Sawdey MS, Keeton MR, Bordin GM, Bernstein EF, Dilley RB, Loskutoff DJ. Increased type 1 plasminogen activator inhibitor gene expression in atherosclerotic human arteries. Proc Natl Acad Sci USA 1992;89:6998–7002.

[35] Gerszten RE, Garcia-Zepeda EA, Lim Y-C, et al. MCP-1 and IL-8 trigger firm adhesion of monocytes to vascular endothelium under flow conditions. Nature 1999;398:718–23.

[36] Apostolopoulos J, Davenport P, Tipping PG. Interleukin-8 production by macrophages from atheromatous plaques. Arterioscler Thromb Vasc Biol 1996;16:1007–12.

[37] Claise C, Edeas M, Chalas J, Cockx A, Abella A, Capel L, Lindenbaum A. Oxidized low-density lipoprotein induces the production of interleukin-8 by endothelial cells. FEBS Lett 1996;398:223–7.

[38] Oemar BS, Werner A, Garnier J-M, et al. Human connective tissue growth factor is expressed in advanced atherosclerotic lesions. Circulation 1997;95:831–9.
[39] Hishikawa K, Oemar BS, Tanner FC, Nakaki T, Fujii T, Luscher TF. Overexpression of connective tissue growth factor gene induces apoptosis in human aortic smooth muscle cells. Circulation 1999;100:2108–12.
[40] Babic AM, Kireeva ML, Kolesnikova TV, Lau LF. CYR61, a product of a growth factor-inducible immediate early gene, promotes angiogenesis and tumor growth. Proc Natl Acad Sci USA 1998;95:6355–60.
[41] Shanahan CM, Cary NRB, Metcalfe JC, Weissberg PL. High expression of genes for calcification-regulating proteins in human atherosclerotic plaques. J Clin Invest 1994;93:2393–402.

EMBO *reports*

scientific report

Use of stepwise subtraction to comprehensively isolate mouse genes whose transcription is up-regulated during spermiogenesis

Takayuki Fujii[1], Kazutoshi Tamura[1], Kumiko Masai[2], Hiromitsu Tanaka[2], Yoshitake Nishimune[2] & Hiroshi Nojima[1,+]

Departments of [1]Molecular Genetics and [2]Science for Laboratory Animal Experimentation, Research Institute for Microbial Diseases, Osaka University, 3-1 Yamadaoka, Suita, Osaka 565-0871, Japan

Received September 19, 2001; revised and accepted February 21, 2002

We report the isolation of 153 mouse genes whose expression is dramatically up-regulated during spermiogenesis. We used a novel variation of the subtractive hybridization technique called stepwise subtraction, wherein the subtraction process is systematically repeated in a stepwise manner. We named the genes thus identified as *TISP* genes (transcript induced in spermiogenesis). The transcription of 80 of these *TISP* genes is almost completely specific to the testis. This transcription is abruptly turned on after 17 days of age, when the mice enter puberty and spermiogenesis is initiated. Considering that the most advanced cells present at these stages of spermatogenesis are the spermatids, it is likely that we could isolate most of the spermatid-specific genes. DNA sequencing revealed that about half the *TISP* genes are novel and uncharacterized genes, confirming the utility of the stepwise subtraction approach for gene discovery.

INTRODUCTION

Spermatogonia are derived from the primordial germ cells through a process called spermatogenesis. Male gametes (sperm) subsequently differentiate from the spermatogonia. The first step in spermatogenesis is the arrival of primordial germ cells at the embryonic genital ridge. These germ cells then become incorporated into the sexual cords, which hollow out upon maturity to form seminiferous tubules, the sites of sperm production in the testis. Sertoli cells, which nourish and protect the developing sperm cells, then differentiate from the epithelium of the somatic cell component of the tubules. The ability to identify these developmental stages by microscopic observation allows us to determine precisely when a gene is expressed during development. This means that spermatogenesis is an excellent model system for the identification of the molecular mechanisms that regulate germ-cell differentiation (Hecht, 1998).

Spermatogenesis in the adult animal can be subdivided into three stages. First, after many rounds of mitotic division, the spermatogonia enter meiosis and thus generate the primary spermatocytes. Secondly, the primary spermatocytes undergo two consecutive meiotic divisions and produce four round spermatids. Thirdly, spermiogenesis, which consists of a series of complex morphogenetic events, occurs. This process lasts ~2 weeks in the mouse and results in the round haploid spermatids developing into morphologically and functionally differentiated spermatozoa. The various morphogenetic events in spermatogenesis appear to be regulated by the organized stage- and cell-specific gene expression in both the germ cells and the supporting somatic cells (Eddy *et al.*, 1993; Eddy and O'Brien, 1998; Hecht, 1998).

During spermiogenesis, histones and non-histone proteins are replaced successively by basic proteins, which are known in round spermatids as transition proteins and in elongating spermatids as protamines (Balhorn, 1989; Hecht, 1995). The genes for these proteins are transcribed within their respective spermatids. The expression of the protamines generates a compacted DNA–protamine complex that may help to safely store chromosomes in the heads of spermatozoa. The complex is also believed to inactivate the transcription of most genes during mid-spermiogenesis (Kierszenbaum and Tres, 1978; Hecht, 1995; Steger, 1999).

+Corresponding author. Tel: +81 6 6875 3980; Fax: +81 6 6875 5192; E-mail: hnojima@biken.osaka-u.ac.jp

The list of genes that are expressed specifically in the mammalian testis is rapidly growing. However, relatively few of these genes have been found to play specific roles in the meiotic phase of spermatogenesis in mammals, and even fewer have been shown to participate in spermiogenesis alone (Eddy and O'Brien, 1998). To identify on a comprehensive scale those genes whose expression is dramatically up-regulated during spermiogenesis, we prepared a subtracted mouse cDNA library enriched in spermiogenesis-specific genes. This was done by using cDNA derived from the testes of adult mice as a tracer and mRNA from the testes of juvenile mice as a driver, given that the haploid spermatid cells are produced only in the adult testes. We then tried to isolate essentially all the genes that are expressed specifically during spermiogenesis in the subtracted cDNA library by a novel variation of the subtraction technique called 'stepwise subtraction', in which the subtraction process is systematically repeated in a stepwise manner. This allowed us to isolate 153 mouse genes. DNA sequencing showed that many are uncharacterized novel genes. Of these, 80 genes seem to be specifically expressed during the latter phase of spermatogenesis (spermiogenesis). These observations indicate that our technique is useful for gene discovery.

RESULTS

Stepwise subtraction to isolate genes whose transcription is specifically induced during spermiogenesis

In the present study, we first prepared a cDNA library from adult testes of 35-day-old mice and subtracted it with mRNA from the testes of juvenile (17-day-old) mice. Northern blot analysis indicated that ~30% of the cDNA clones in the subtracted library were expressed more intensely in the adult testes than in the juvenile testes. These bands could be classified into three types based on the pattern of band intensity (Figure 1A). Type 1 clones showed no expression in the juvenile testis, whereas the expression intensity in the adult testis was very strong. Type 2 clones showed an intense expression in the adult testis, but weak expression in the juvenile testis was also observed. Type 3 clones showed at least two bands, the intensity of one being almost equal in the juvenile and adult testes and the other being found predominantly in the adult testis. We have named all these cDNA clones as *TISP* clones (transcript induced in spermiogenesis). To assess the effect of the stepwise subtraction on our ability to identify all the potential *TISP* genes in the library, we plotted the number of *TISP* clones that were successfully identified at each hybridization step against the total number that had been tested by each step. In the absence of stepwise subtraction, one would see the harvest curve gradually falling and then flattening as the number on the abscissa increases (Figure 1B). Actually, when we plotted the harvest curve for Type 1, 2 and 3 clones isolated at the first subtraction step against the total clones analyzed, we observed a flattened curve in all three cases (Figure 1C). Thus, in the screen of the first-stage subtracted cDNA library, we isolated 31, 11 and seven Type 1, 2 and 3 clones, respectively.

When the stepwise subtraction was performed on the first-stage subtracted cDNA library to circumvent the redundant isolation of cDNA clones (see Methods), the harvest curve again started to increase, gradually falling and then flattened. Thus, in the screen of the second-stage subtracted cDNA library, we could isolate another 33 Type 1, 13 Type 2 and 10 Type 3 clones. Similarly, we performed the stepwise subtractions repeatedly to make the fifth-stage subtracted cDNA library and had isolated a total of 80 Type 1, 41 Type 2 and 32 Type 3 cDNA clones. Indicating the success of the five stepwise subtractions in isolating most of the *TISP* clones in the original library, only 32 of the 320 randomly selected clones in the fifth-stage subtracted cDNA library were unique clones (as assessed by Southern blot analysis), and only three Type 1, one Type 2 and three Type 3 cDNA clones were isolated. This suggests that, by the fifth-stage subtraction, we had isolated almost all of the *TISP* clones present in the first-stage subtracted cDNA library.

Developmental and tissue-specific expression of *TISP* cDNA clones

The cDNA inserts in the isolated *TISP* clones were cut out by digestion with *Sma*I and *Not*I restriction enzymes and labeled with ^{32}P. These probes were used for northern blot analysis. Northern blots of the RNA from mouse testis of various ages indicates that expression of all Type 1 *TISP* genes is very low in the pre-pubertal testis (2–5, 8 and 17 days old) but that transcription of these genes is abruptly induced in the post-pubertal testis (23 days old) and is increased further in the testes of 29-day-old mice (Figure 2). Spermiogenesis occurs only in the postpubertal testis, which suggests that the transcription of many of the Type 1 *TISP* genes is induced during spermiogenesis. Indeed, northern blot analysis of fractionated samples and *in situ* hybridization analyses confirm that the transcription of all Type 1 *TISP* genes examined to date is induced in the germ cells of the postpubertal testis during spermiogenesis (Fujii *et al.*, 1999; Iguchi *et al.*, 1999; Koga *et al.*, 2000; Tosaka *et al.*, 2000; Yamanaka *et al.*, 2000; Carvalho *et al.*, 2002). Northern blot analysis for Type 2 and 3 *TISP* clones indicate that their expression is not specific to the postpubertal testis during spermiogenesis (see Supplementary figure available at *EMBO reports* Online). In fact, some of them are expressed even in the infant testis (data not shown), making these clones less interesting for our purposes than the Type 1 *TISP* clones.

As shown in Figure 2, northern blots using RNA isolated from various murine tissues indicate that all Type 1 *TISP* clones are expressed predominantly in the testis—except for *TISP12*, which is also expressed in other tissues (Yamanaka *et al.*, 2000). This suggests that most Type 1 *TISP* genes function specifically in the testis. *TISP14* and *TISP44* are exceptional, in the sense that they are also expressed in the ovary, suggesting that they may also play a role in the development of the female gonad. Type 2 and 3 *TISP* genes appear to be expressed in other tissues as well as in the testis, again making them less interesting (data not shown).

We also analyzed the transcription of *TISP* clones by northern blot analysis with RNA from testes that cannot produce differentiated germ cells, such as those in cryptorchid (Nishimune *et al.*, 1981), *jsd/jsd* (Mizunuma *et al.*, 1992; Kojima *et al.*, 1997), Sl^{17H}/Sl^{17H} (Brannan *et al.*, 1992 and W/W^{v} mice (Yoshinaga *et al.*, 1991) (Figure 2). As expected, all Type 1 *TISP* genes are expressed at almost undetectable levels in these testes, further emphasizing the specific role these genes play in spermiogenesis.

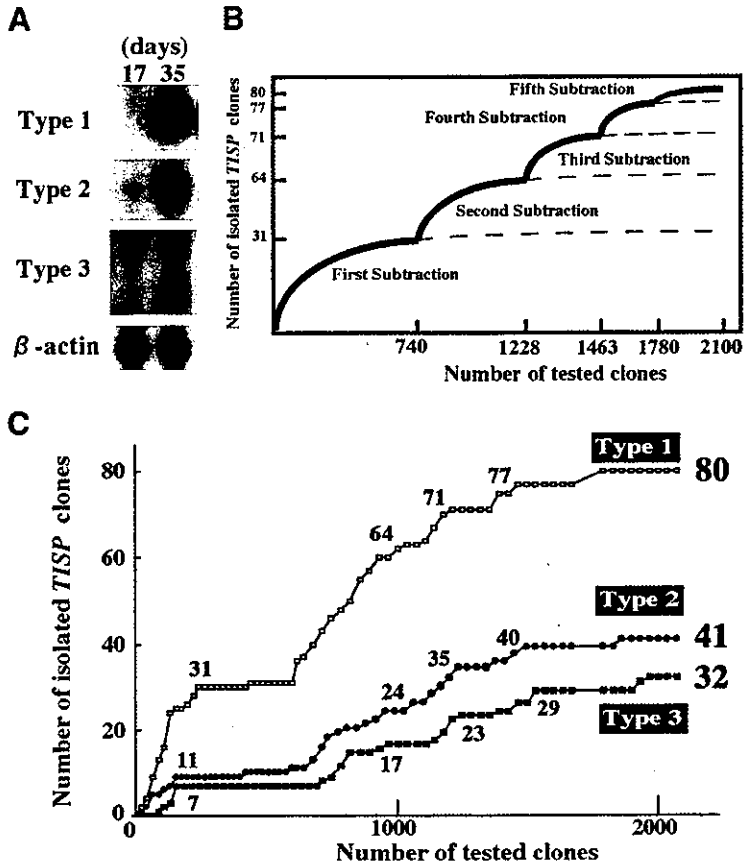

Fig. 1. A stepwise subtraction strategy for comprehensively isolating genes whose transcription is induced during spermiogenesis. (**A**) The *TISP* cDNA clones obtained by stepwise subtraction can be classified into three types according to the pattern of band intensity in northern blots with juvenile and adult testicular RNA. A northern blot with radiolabeled β-actin cDNA is shown as a loading control. See text for details. (**B**) The effect of the stepwise subtractions on the total harvest of *TISP* clones from the cDNA library can be monitored by plotting the total number of non-redundant cDNA clones analyzed after each stage (abscissa) against the number of *TISP* cDNA clones that were isolated in each stage (ordinate). The shapes of the harvest curve that might be drawn without performing the stepwise subtractions are shown by broken lines. (**C**) The actual harvest curve for each type of *TISP* cDNA clone resulting from performing the five stepwise subtractions. The isolated *TISP* clones are divided into the three classes. Numbers shown at each node of the curves signify the total number of *TISP* cDNA clones isolated by the end of each subtraction step. The nodes represent the five hybridizations that were performed on the cDNA library.

Many of the *TISP* genes are novel and uncharacterized

DNA sequencing of these genes showed that 30 Type 1, 12 Type 2 and 10 Type 3 *TISP* genes are identical to the registered genes in the DNA data bank. Of the remaining genes, 12 Type 1, five Type 2 and two Type 3 genes are homologous to previously characterized genes (see Supplementary table). The other 38 Type 1, 24 Type 2 and 20 Type 3 *TISP* genes are novel and uncharacterized genes. The previously characterized genes include protamine 1 (*TISP18*), protamine 2 (*TISP1*) and transition protein 2 (*TISP28*), all of which are known to play pivotal roles in spermiogenesis (Eddy and O'Brien, 1998; Hecht, 1998). We also encountered genes known to be expressed in a testis-specific manner, including testis-specific phosphoglycerate kinase (*TISP4*), sperm mitochondrial capsule protein (*TISP11*), cystatin-related epidermal spermatogenic protein (*TISP14*), actin-like-7 α and β proteins (*TISP61* and *TISP19*), sperm-egg recognition protein precursor (*TISP29*), substrate for testis-specific serine kinases Tssk-1 (*TISP37*) and Tssk-2 (*TISP47*), testis-specifically expressed cDNAs-2 (Tsec-2; *TISP60*) and DNA binding protein Hils1 (*TISP64*) (Eddy *et al.*, 1993; Eddy and O'Brien, 1998; Chadwick *et al.*, 1999). Interestingly, we also isolated the genes for fibrous sheath component (*TISP52*) and tektin (*TISP76*), which are potential constituents of the sperm tail (Iguchi *et al.*, 1999). In addition, we identified a splicing isoform of phospholipase C delta 4 (PLC-δ4; *TISP30*) that is known to be predominantly expressed in the testis and was recently found to function in the acrosome reaction, an exocytotic event required for fertilization (Fukami *et al.*, 2001). These results indicate that the strategy and techniques we used were successful in isolating, on a comprehensive scale, spermiogenesis-specific genes.

DISCUSSION

In the present study, we report the comprehensive isolation of cDNA clones that putatively encode mouse haploid germ-cell-specific proteins by preparing a spermiogenesis-specific subtracted cDNA library. This library was subjected to a novel variation of the hybridization technique called stepwise subtraction

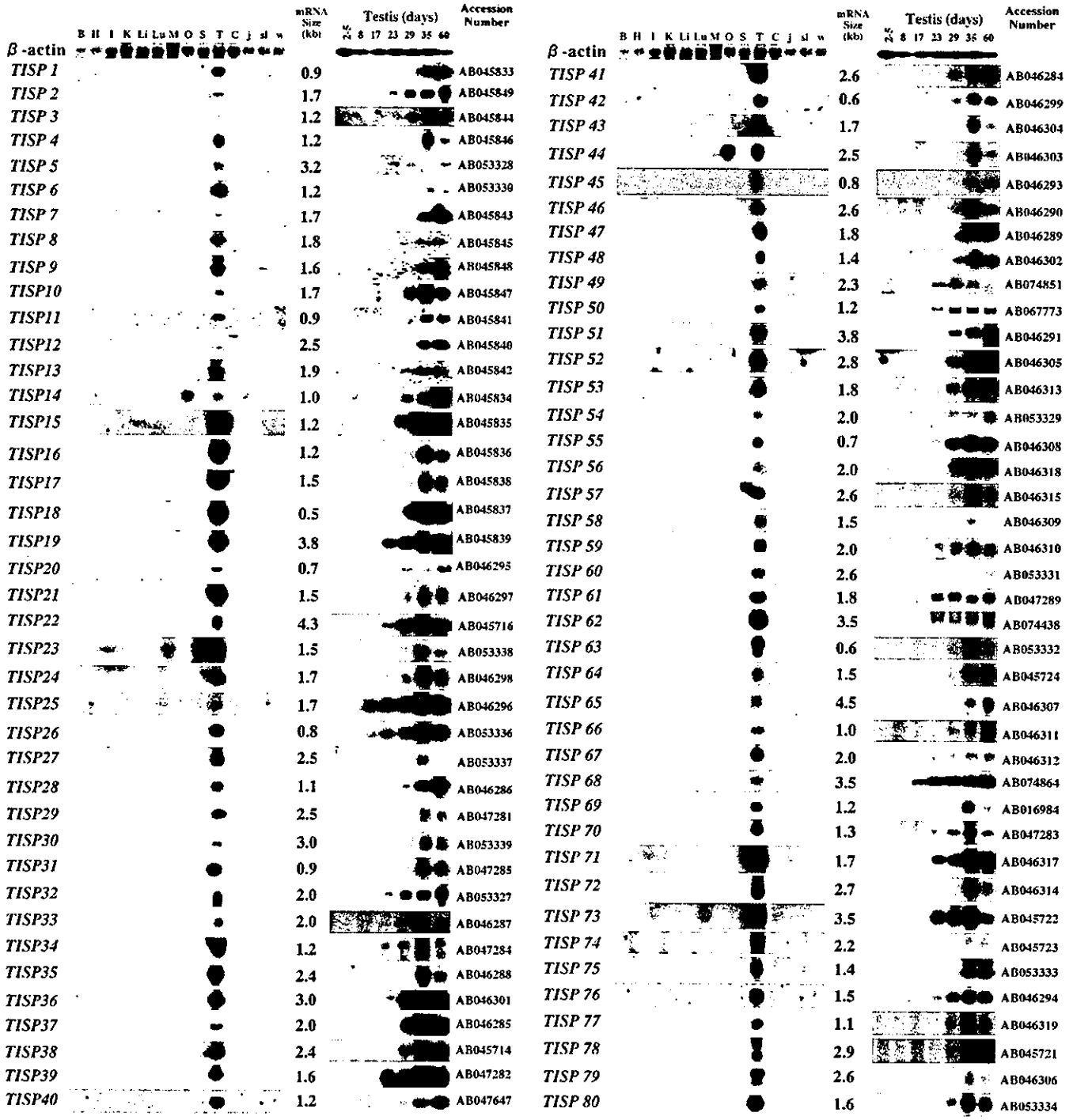

Fig. 2. Expression of each Type 1 *TISP* cDNA clone. Northern blot analysis was performed by hybridizing the radiolabeled cDNA insert of each *TISP* clone to RNA from various murine tissues, from the testes of four kinds of mutant mice or from the testes of mice of varying ages. B, brain; H, heart; I, intestine; K, kidney; Li, liver; Lu, lung; M, skeletal muscle; O, ovary; S, spleen; T, testis; C, cryptorchid testis; j, testis of *jsd/jsd* mouse at 3 months of age; sl, testis of Sl^{17H}/Sl^{17H} mouse; w, testis of W/W^{v} mouse. The number shown at the right of each blot denotes the size of the mRNA as assessed by the RNA size marker run in a parallel lane of each agarose gel (not shown). A northern blot with radiolabeled β-actin cDNA is shown as a loading control. The accession number for each *TISP* cDNA sequence (registered in the DDBJ data bank) is shown beside each northern blot.

(Figure 1), which allowed us to efficiently isolate 153 genes whose transcription is induced during the spermatogenesis. Among these genes are the 80 so-called Type 1 *TISP* genes, whose expression is dramatically up-regulated during spermiogenesis in a plus/minus manner. Northern blot analysis during male germ-cell development indicates that the mRNA of these

Type 1 *TISP* genes is detected predominantly in the normal mouse testis but not in the testes of mutant mice known to lack differentiated germ cells in the testis (Figure 2). In addition, it appears that the transcription of all the Type 1 *TISP* genes is abruptly induced after 17 days of age, at which time spermiogenesis is initiated. This testis-specific expression at the point in development when transcription begins strongly suggests that the 80 *TISP* genes we identified play major physiological roles in the regulation of spermiogenesis.

DNA sequencing indicated that many of the *TISP* genes we isolated are novel (see Supplementary table). We analyzed the expression of some of the *TISP* genes in more detail by northern blot analysis. This indicated that the *TISP14* and *TISP44* genes are expressed predominantly in both the testis and ovary, suggesting that these *TISP* genes may be pivotal in both male and female gametogenesis (Figure 2). *TISP10, TISP12, TISP15, TISP50, TISP69* and *TISP76* genes also showed developmental stage- and location-specific expression (Fujii *et al.*, 1999; Iguchi *et al.*, 1999; Koga *et al.*, 2000; Tosaka *et al.*, 2000; Yamanaka *et al.*, 2000; Carvalho *et al.*, 2002) and may be involved in processes such as supplying energy for sperm motility (*TISP12*; Yamanaka *et al.*, 2000) and the regulation of polyamine levels in male haploid germ cells (*TISP15*; Tosaka *et al.*, 2000). Further detailed functional analysis of these novel *TISP* genes will dramatically expand the current understanding of spermiogenesis at the molecular level.

Recently, it was reported that the X chromosome plays a prominent role in the pre-meiotic stages of mammalian spermatogenesis because, of the 25 genes that are expressed specifically in mouse spermatogonia, three are Y-linked and 10 are X-linked (Wang *et al.*, 2001). However, the chromosomal localizations of *TISP* genes and some of the haploid-specific genes in the mouse genome (Yoshimura *et al.*, 2001), and the chromosomal positions of the human *TISP* homologs by using the BLAST network service of NCBI for human genome sequencing (data not shown), indicates that they are scattered throughout the genome and are present on autosomes as well as sex chromosomes. Thus, *TISP* genes do not appear to be preferentially localized on sex chromosomes.

METHODS

Preparation and analysis of the subtracted cDNA library. An adult testis cDNA library with 2 million independent clones was constructed from 35-day-old mice using the linker-primer method with a pAP3neo vector as described previously (Kobori *et al.*, 1998; Fujii *et al.*, 1999). We next prepared mRNA from the testes of juvenile mice (17 days old) and biotinylated the mRNA with photobiotin. After converting the cDNA library into a single-stranded form by transfection with f1 helper phage, we hybridized it with the biotinylated mRNA and subtracted it by biotin–avidin interaction as described previously (Kobori *et al.*, 1998). The unhybridized clones were converted to the double-stranded form, which was then used to transform competent *Escherichia coli* cells, generating a subtracted cDNA library of 20 000 independent clones.

To analyze the quality of this first-stage subtracted cDNA library, we prepared plasmid DNA from 740 randomly selected cDNA clones and digested an aliquot of each plasmid DNA with *Sma*I and *Not*I restriction enzymes to prepare 10 sheets of Southern blots, each of which included 80 clones arranged in order. We also purified the cDNA inserts of clones 1–20 on 1% agarose gels by digesting them with *Eco*RI and *Not*I, and they were then ^{32}P-labeled to use as probes not only for Southern blot analysis to find redundant clones but also for northern blot analysis to identify *TISP* clones. Each northern sheet included only two lanes—one each with the RNA extracted from the testes of juvenile (17-day-old) and adult (35-day-old) mice (Figure 1A). The DNA sequences of the *TISP* clones were determined from the 5′ end of the cDNA inserts by the dideoxy-chain termination reaction using an automatic DNA sequencer (Licor 4000L, Lincoln, NE). After these analyses, we selected 20 unhybridized clones by Southern blot analysis (from 21) for the next round of cDNA insert preparation, radiolabeling and northern/Southern blot analysis. This procedure was repeated until we had finished selecting all the unhybridized cDNAs of the 740 clones in Southern blot analysis. In all, we subjected 169 clones to northern/Southern blot analysis.

Stepwise subtraction of the cDNA library. After DNA sequencing of the first-stage subtracted cDNA library, we collected 0.1 μg of each of the 169 plasmid DNAs into one tube, mixed and digested the DNA with *Not*I and subjected 5 μg to a T7 RNA polymerase reaction to convert the cDNA inserts into the RNA form. The reaction mixture was treated with 70 U of DNase I to remove the DNA substrate. The generated RNA was biotinylated using Photoprobe biotin (Vector Laboratories, Burlingame, CA) and mixed with the single-stranded DNA (ssDNA) form of the first-stage subtracted cDNA library in 25 μl total volume of hybridization mixture containing 40% formamide, 50 mM HEPES pH 7.5, 1 mM EDTA, 0.1% SDS and 0.2 M NaCl. In addition, 1 μg of masking oligonucleotide (5′-CCCGGGG-ATCTAGACGTCGAATTCCC-3′) was added to the mixture to prevent non-specific hybridization via the junctional region between the pAP3neo vector and the cDNA inserts. The reaction mixture was then placed in a FUNA-PCR tube (Funakoshi, Tokyo), heated to 65°C for 10 min and incubated at 42°C for 48 h to allow hybridization between the RNA and ssDNA. After hybridization, we used a modified streptavidin–phenol/chloroform extraction protocol (Sive and St John, 1988) as reported previously (Kobori *et al.*, 1998). The subtracted ssDNA was recovered and converted to the double-stranded form with *Bca*BEST DNA polymerase (TaKaRa, Tokyo, Japan) as described previously (Kobori *et al.*, 1998). This double-stranded plasmid DNA was used to transform competent *E. coli* cells by electroporation (Kobori and Nojima, 1993), generating the second-stage subtracted cDNA library, which contained ~2.0×10^4 independent clones. From this second-stage subtracted cDNA library, we randomly selected 488 clones for plasmid DNA preparation and subjected 259 of them to northern/Southern blot analysis.

To prepare the third-stage subtracted library, we collected 0.1 μg of plasmid DNA from each of the 259 clones, converted them into the RNA form and hybridized with the ssDNA form of the second-stage subtracted cDNA library as described above. To identify novel *TISP* clones, we randomly selected 235 for plasmid DNA preparation and subjected 84 clones to northern/Southern blot analysis. This procedure was repeated until we obtained a fifth-stage subtracted library. During this process, we randomly selected 317 and 320 clones for plasmid DNA preparation from the fourth- and fifth-stage subtracted libraries, respectively, to identify novel *TISP* clones and subjected 110

and 32 clones to northern and Southern blot analysis, respectively. To prepare the fourth- and fifth-stage subtracted libraries, we collected 0.1 μg of plasmid DNA for each of 84 and 110 clones, respectively, to convert into RNA form for subtractive hybridization. The third-, fourth- and fifth-stage subtracted cDNA libraries contained ~1.0×10^4, 1.4×10^4, and 1.2×10^4 independent clones, respectively.

Northern blot analysis. The preparation of RNA from various tissues, the fractionation of germ, Leydig and Sertoli cells from adult mice and northern blot analysis were all performed as described previously (Iguchi *et al.*, 1999; Koga *et al.*, 2000). The cDNA inserts cut out of the plasmids by the *Sma*I and *Not*I restriction enzymes were radiolabeled with [^{32}P]dCTP using the Random Primer DNA Labeling kit (TaKaRa) and used as hybridization probes.

Supplementary data. Supplementary data are available at *EMBO reports* Online.

ACKNOWLEDGEMENTS

We thank Dr P. Hughes for critically reading the manuscript. We also thank Mr I. Nagamori for technical assistance. This work was supported by a Grant-in-aid for Scientific Research on Priority Areas from the Ministry of Education, Science, Sports and Culture of Japan and a grant from The Uehara Memorial Foundation (to H.N.).

REFERENCES

Balhorn, R. (1989) Mammalian protamines: structure and molecular interactions. In Adolph, K.W. (ed.), *Molecular Biology of Chromosome Function*. Springer, New York, NY, pp. 366–395.

Brannan, C.I. *et al.* (1992) Developmental abnormalities in Steel 17H mice result from a splicing defect in the steel factor cytoplasmic tail. *Genes Dev.*, **10**, 1832–1842.

Carvalho, C.E., Tanaka, H., Iguchi, N., Ventelä, S., Nojima, H. and Nishimune, Y. (2002) *Biol. Reprod.*, **66**, in press.

Chadwick, B.P. *et al.* (1999) Cloning, mapping, and expression of two novel actin genes, actin-like-7A (ACTL7A) and actin-like-7B (ACTL7B), from the familial dysautonomia candidate region on 9q31. *Genomics*, **58**, 302–309.

Eddy, E.M. and O'Brien, D.A. (1998) Gene expression during mammalian meiosis. In Handel, M.A. (ed.), *Meiosis and Gametogenesis*. Academic Press, London, UK, pp. 141–200.

Eddy, E.M., Welch, J.E. and O'Brien, D.A. (1993) Gene expression during spermatogenesis. In de Kretser, D.M. (ed.), *Cellular and Molecular Mechanisms in Male Reproduction*. Academic Press, London, UK, pp. 181–232.

Fujii, T. *et al.* (1999) Sperizin is a murine RING zinc finger protein specifically expressed in haploid germ cells. *Genomics*, **57**, 94–101.

Fukami, K. *et al.* (2001) Requirement of phospholipase Cdelta4 for the zona pellucida-induced acrosome reaction. *Science*, **292**, 920–923.

Hecht, N.B. (1995) The making of a spermatozoon: a molecular perspective. *Dev. Genet.*, **16**, 95–103.

Hecht, N.B. (1998) Molecular mechanisms of male germ cell differentiation. *BioEssays*, **20**, 555–561.

Iguchi, N., Tanaka, H., Fujii, T., Tamura, K., Kaneko, Y., Nojima, H. and Nishimune, Y. (1999) Molecular cloning of haploid germ cell-specific tektin cDNA and analysis of the protein in mouse testis. *FEBS Lett.*, **456**, 315–321.

Kierszenbaum, A.L. and Tres, L.L. (1978) RNA transcription and chromatin structure during meiotic and postmeiotic stages of spermatogenesis. *Fed. Proc.*, **37**, 2512–2516.

Kobori, M. and Nojima, H. (1993) A simple treatment of DNA in a ligation mixture prior to electroporation improves transformation frequency. *Nucleic Acids Res.*, **21**, 2782.

Kobori, M., Ikeda, Y., Nara, H., Kato, M., Kumegawa, M., Nojima, H. and Kawashima, H. (1998) Large scale isolation of osteoclast-specific genes by an improved method involving the preparation of a subtracted cDNA library. *Genes Cells*, **3**, 459–475.

Koga, M. *et al.* (2000) Isolation and characterization of a haploid germ cell-specific novel complementary deoxyribonucleic acid; testis-specific homologue of succinyl CoA:3-Oxo acid CoA transferase. *Biol. Reprod.*, **63**, 1601–1609.

Kojima, Y., Kominami, K., Dohmae, K., Nonomura, N., Miki, T., Okuyama, A., Nishimune, Y. and Okabe, M. (1997) Cessation of spermatogenesis in juvenile spermatogonial depletion (jsd/jsd) mice. *Int. J. Urol.*, **4**, 500–507.

Mizunuma, M., Dohmae, K., Tajima, Y., Koshimizu, U., Watanabe, D. and Nishimune, Y. (1992) Loss of sperm in juvenile spermatogonial depletion (*jsd*) mutant mice is ascribed to a defect on intratubular environment to support germ cell differentiation. *J. Cell Physiol.*, **150**, 188–193.

Nishimune, Y., Haneji, T. and Aizawa, S. (1981) Testicular DNA synthesis *in vivo*: changes in DNA synthetic activity following artificial cryptorchidism and its surgical reversal. *Fertil. Steril.*, **35**, 359–362.

Sive, H.L. and St John, T. (1988) A simple subtractive hybridization technique employing photoactivatable biotin and phenol extraction. *Nucleic Acids Res.*, **16**, 10937.

Steger, K. (1999) Transcriptional and translational regulation of gene expression in haploid spermatids. *Anat. Embryol.*, **199**, 471–487.

Tosaka, Y., Tanaka, H., Yano, Y., Masai, K., Nozaki, M., Yomogida, K., Otani, S., Nojima, H. and Nishimune, Y. (2000) Identification and characterization of testis specific ornithine decarboxylase antizyme (OAZ-t) gene: expression in haploid germ cells and polyamine-induced frameshifting. *Genes Cells*, **5**, 265–276.

Wang, P.J., McCarrey, J.R., Yang, F. and Page, D.C. (2001) An abundance of X-linked genes expressed in spermatogonia. *Nature Genet.*, **27**, 422–426.

Yamanaka, M. *et al.* (2000) Molecular cloning and characterization of phosphatidylcholine transfer protein-like protein gene expressed in murine haploid germ cells. *Biol. Reprod.*, **62**, 1694–7101.

Yoshimura, Y., Tanaka, H., Nozaki, M., Yomogida, K., Yasunaga, T. and Nishimune, Y. (2001) Nested genomic structure of haploid germ cell specific haspin gene. *Gene*, **267**, 49–54.

Yoshinaga, K., Nishikawa, S., Ogawa, M., Hayashi, S.-I., Kunisada, T., Fujimoto, T. and Nishikawa, S.-I. (1991) Role of *c-kit* in mouse spermatogenesis: identification of spermatogonia as a specific site of *c-kit* expression and function. *Development*, **113**, 689–699.

DOI: 10.1093/embo-reports/kvf073

Experimental Cell Research 279, 91–99 (2002)
doi:10.1006/excr.2002.5590

Suppression of Anchorage-Independent Growth of Human Cancer Cell Lines by the TRIF52/Periostin/OSF-2 Gene

Naohisa Yoshioka,* Shigeo Fuji,* Misuzu Shimakage,† Ken Kodama,‡ Akira Hakura,‖ Masuo Yutsudo,§ Hirokazu Inoue,[1] and Hiroshi Nojima*,[1]

*Department of Molecular Genetics, §Department of Bacterial Infections, and ‖Department of Tumor Virology, Research Institute for Microbial Diseases, Osaka University, Suita 565-0871, Japan; †Clinical Research Institute, Osaka National Hospital, Osaka 540-0006, Japan; ‡Department of Thoracic Surgery, Osaka Medical Center for Cancer and Cardiovascular Diseases, Osaka 537-8511, Japan; and [1]Department of Microbiology, Shiga University of Medical Science, Otsu 520-2192, Japan

In searching for genes that suppress the viral transformation of primary cells, we have isolated a number of TRIF (transcript reduced in F2408) genes that are expressed well in primary rat embryo fibroblasts (REFs) but poorly in spontaneously immortalized rat fibroblast cell lines derived from REFs. One of these genes, TRIF52, is a rat homologue of the mouse protein periostin, which is suspected of being involved in oncogenesis. We found here that periostin mRNA expression is markedly downregulated in a variety of human cancer cell lines and human lung cancer tissues. Human cancer cell lines with reduced endogenous periostin gene expression that were infected with a recombinant retrovirus containing the periostin gene had reduced anchorage-independent growth. Mutational analysis revealed that the C-terminal region of periostin is sufficient to convey the anchorage-independent growth-suppressive activity of the protein. These observations together suggest that periostin may serve to inhibit the development of human cancers by acting as a tumor suppressor.

Key Words: **periostin; tumor suppression; anchorage-independent growth; primary cells; transformation.**

INTRODUCTION

We have reported previously that factors that suppress transformation by viral oncogenes are expressed in primary rat embryo fibroblasts (REFs) [1]. To identify such transformation suppressor genes, we used cDNA subtraction to isolate 30 different cDNA clones whose mRNA expression is markedly reduced in the rat fibroblast cell line F2408 [1]. We referred to these clones as TRIF (transcript reduced in F2408). In a previous article, we demonstrated that TRIF3 (lumican) suppresses transformation by v-*src* and v-K-*ras* oncogenes, which suggests that the other TRIF genes may also be transformation suppressor candidates [1].

In this article, we focus on TRIF52, a rat homologue of mouse periostin. Periostin, formerly called osteoblast-specific factor 2 (osf-2), was previously isolated as an osteoblast-specific gene from a cDNA library of the mouse osteoblastic cell line MC3T3-E1 by subtraction hybridization and differential screening techniques [2]. Periostin has a typical signal peptide sequence at its N terminus and four repeated domains. Each of the latter domains contain two highly conserved sequences that have been found in the fasciclin I family of proteins [2, 3]. Periostin is particularly highly homologous to βig-h3, one of the fasciclin I protein family, which has been isolated as a transforming growth factor β (TGF-β)-responsive gene [4]. βig-h3 promotes the cell adhesion and spreading of fibroblasts via integrin α1β2 [5, 6] but also suppresses the ability of CHO cells to develop into tumors in nude mice [7]. Periostin is also involved in the cell adhesion and spreading of osteoblastic cells [3]. In addition, the protein expression of periostin is increased by TGF-β [3], and mRNA expression of periostin is downregulated by the introduction of Wnt-3 and by the inhibition of glycogen synthase kinase 3β (GSK-3β) [8]. These observations suggest that loss of periostin expression could promote oncogenesis.

To clarify whether periostin/TRIF52 could inhibit human oncogenesis as a tumor suppressor, we investigated the expression of periostin mRNA in a variety of human cancer cell lines and several human lung cancer tissues. We found most tumors poorly expressed periostin mRNA. Furthermore, we tested the ability of exogenous periostin to suppress the malignant phenotype of those human cancer cell lines with a downregulated expression of periostin mRNA. We found that periostin can suppress the anchorage-independent growth of these cells, supporting the notion that periostin has a tumor suppressor function in human oncogenesis.

[1] To whom reprint requests should be addressed. Fax: +81 6 6875 5192. E-mail: hnojima@biken.osaka-u.ac.jp

0014-4827/02 $35.00

MATERIALS AND METHODS

Cells. The human cells used in this study were HEFs (human embryo fibroblasts), KD (normal human fibroblasts), WI38 (normal human fibroblasts), HaCaT (skin keratinocytes), T24 (bladder cancer), SaOS-2 (osteosarcoma), HeLa, CaSki, SiHa and C33A (cervical cancers), S3 (endometrial cancer), G401 (Wilms' tumor), SW837 (colon cancer), HT1080 (fibrosarcoma), A172 (glioblastoma), NB-1 (neuroblastoma), AZ521 (gastric cancer), MeWo (melanoma), MIA-PaCa-2 (pancreatic cancer), RERF-LC-MS, A549, VMRA-LCD, CADO-LC4, CADO-LC29, and CADO-LC46 (lung adenocarcinoma), H69 (small cell lung cancer), and MCF7 (breast cancer). The cells were cultured in Dulbecco's modified Eagle's medium (DMEM) supplemented with 10% fetal bovine serum (FBS).

Construction of retrovirus vectors expressing periostin and deletion mutants. pCXbsr, a Moloney murine leukemia virus (MuLV)-based retrovirus vector containing the blasticidin S resistance gene (bsr) as a selectable marker, was constructed by Akagi *et al.* [9]. The original *Sal*I site in the pCXbsr vector was eliminated by blunt-end ligation after digestion with *Sal*I and a new *Sal*I site was introduced into the multicloning sites between the *Eco*RI and *Not*I sites in the pCXbsr vector. Wild-type periostin and deletion mutants were amplified by polymerase chain reaction (PCR) designed to introduce 5′ *Eco*RI and 3′ *Asc*I sites at either end of these genes. The PCR products were digested with *Eco*RI/*Asc*I and subcloned into the *Eco*RI–*Asc*I sites of the pBlueScript II–hemagglutinin (HA) vector so that the HA gene would be linked to the periostin genes in-frame at the 3′ end. After DNA sequencing, the *Eco*RI/*Sal*I fragments of wild-type (WT) and deletion mutants (ΔN, ΔC, ΔNC, C-term) bearing the HA gene were ligated into the *Eco*RI–*Sal*I sites of the pCXbsr vector. These vectors were designated as pCXbsr/WT, pCXbsr/ΔN, pCXbsr/ΔC, pCXbsr/ΔNC, and pCXbsr/C-term, respectively. GFP-linked periostin constructs (wild type and C-term) were made by changing HA gene for green fluorescence protein (GFP) gene, and ligated into the *Eco*RI–*Not*I sites of pcDNA3 vector.

Production of amphotropic retroviruses. pCXbsr, pCXbsr/WT, pCXbsr/ΔN, pCXbsr/ΔC, pCXbsr/ΔNC, and pCXbsr/C-term were each contransfected with the pCL-Ampho vector (which expresses an amphotropic envelope) into BOSC23 cells by using the Lipofectamine Plus reagent (Life Technologies) according to the manufacturer's protocols. Two days after transfection, the culture supernatants were collected and frozen as viral stocks.

Virus infection of cancer cell lines and soft agar assay. Two hundred thousand cancer line cells were plated on a 60-mm dish and cultured overnight. Culture medium was removed after polybrene treatment (8 μg/ml) for 30 min, and then the cells were incubated with the amphotropic retrovirus for 1 h at 37°C. A day after the infection, cells were selected with blasticidin S (10 μg/ml) for 10 days, and drug-resistant colonies were pooled. Anchorage-independent growth was examined by colony-forming ability in soft agar. Ten thousand cells were inoculated into 0.4% Noble agar containing DMEM supplemented with 10% FBS in a 60-mm dish. After 3 weeks of incubation, the number of colonies (>0.15 mm in diameter) in each plate was scored. Each assay was tested in duplicate dishes in at least three independent experiments.

Northern blot analyses. Total RNA was extracted from cultured cells with guanidine thiocyanate followed by centrifugation in cesium chloride solution, and poly(A)$^+$ RNA was purified from total RNA by oligo(dT)-Latex chromatography (Nippon Roche Ltd. Tokyo, Japan). Poly(A)$^+$ RNA or total RNA was separated by electrophoresis on a 1% agarose gel containing formaldehyde and transferred to a Biodyne A nylon membrane (PALL BioSupport, NY) in 20× SSC. The human or rat periostin cDNA was labeled with [α-^{32}P]dCTP (ICN Biomedicals Inc.) using a Multiprime DNA labeling system (Amersham Pharmacia Co., Buckinghamshire, England) and used for hybridization as probes. To assess the periostin mRNA expression in normal human and rat tissues, we used poly(A)$^+$ RNA multiple tissue Northern blots purchased from Clontech.

RT-PCR analysis. Total RNA was isolated from cultured cells as described above. Reverse transcription (RT) and PCR amplification was performed by use of a OneStep RT-PCR kit (Qiagen) according to the manufacturer's instructions with minor modifications. Two-tenths microgram of total RNA was used for reverse transcription. The sequences of the RT-PCR primers are as follows: the forward primer for periostin, 5-GACTCAAGATGATTCCCTTT-3′; the reverse primer for periostin, 5-GGTGCAAAGTAAGTGAAGGA-3′; the forward primer for β-actin, 5-AACCGCGAGAAGATGACCCAGAT-3′; the reverse primer for β-actin, 5-GAAGGAAGGTTGGAAGAGAGCCT-3′. PCR was performed for 30 cycles consisting of denaturation at 94°C for 30 s, annealing at 60°C for 30 s, and extension at 72°C for 30 s, followed by a final extension for 7 min. PCR products were separated by electrophoresis on a 2% agarose gel and stained with ethidium bromide.

Immunoblotting. Cells were lysed with RIPA buffer containing 0.15 M NaCl, 50 mM Tris–HCl (pH 7.5), 1 mM EDTA, 1% Triton X-100, 1% sodium deoxycholate, 0.1% SDS, 100 μg/ml PMSF, and 1 μg/ml aprotinin. Cell lysates (500 μg protein/sample) from T24 cells were immunoprecipitated with anti-HA antibody (polyclonal, MBL, Nagoya, Japan) to concentrate the HA-tagged periostin protein. The immune complexes or an equal amount of each cell lysate was subjected to 10% SDS–polyacrylamide gel electrophoresis (SDS-PAGE), and electroblotted onto a PVDF membrane. The membrane was incubated successively with either rat monoclonal antibody (3F10, Boehringer-Mannheim) or mouse monoclonal antibodies (16B12, BAbCO) specific for HA, and then horseradish peroxidase-conjugated anti-rat or -mouse IgG (Amersham). Protein bands were visualized using the ECL reagent.

In situ mRNA hybridization. *In situ* mRNA hybridization was performed on formalin-fixed paraffin sections as described previously [10]. Briefly, the deparaffinized sections were hybridized with a digoxigenin-labeled antisense or sense riboprobe of periostin cDNA at 37°C for 48 h and then incubated with alkaline phosphatase-conjugated anti-digoxigenin antibody at room temperature for 2 h. Signals were visualized by incubation with nitroblue tetrazolium and X-phosphate at 37°C for 2 h.

RESULTS

Periostin mRNA Expression Is Downregulated in Human Cancer Cell Lines and Lung Cancer Tissues

The search for potential transformation suppressor genes in REFs by cDNA subtraction previously revealed that, compared with REFs, expression of periostin/TRIF52 is markedly reduced in rat cell lines such as F2408, 3Y1, 67I, and 67T [1]. To assess whether periostin could also have a tumor suppressor function in human carcinogenesis, we used Northern blot analysis to examine the expression of periostin mRNA in normal human and rat tissues and in human cancer cell lines and tissues. As shown in Fig. 1A, periostin expression was detected in most of the normal human tissues examined except for the spleen and peripheral blood leukocytes. In particular, the periostin mRNA was highly expressed in the heart, placenta, and stomach. With respect to rat tissues, periostin mRNA was detected in all tissues examined and in particular was highly expressed in the lung (Fig. 1B). That periostin

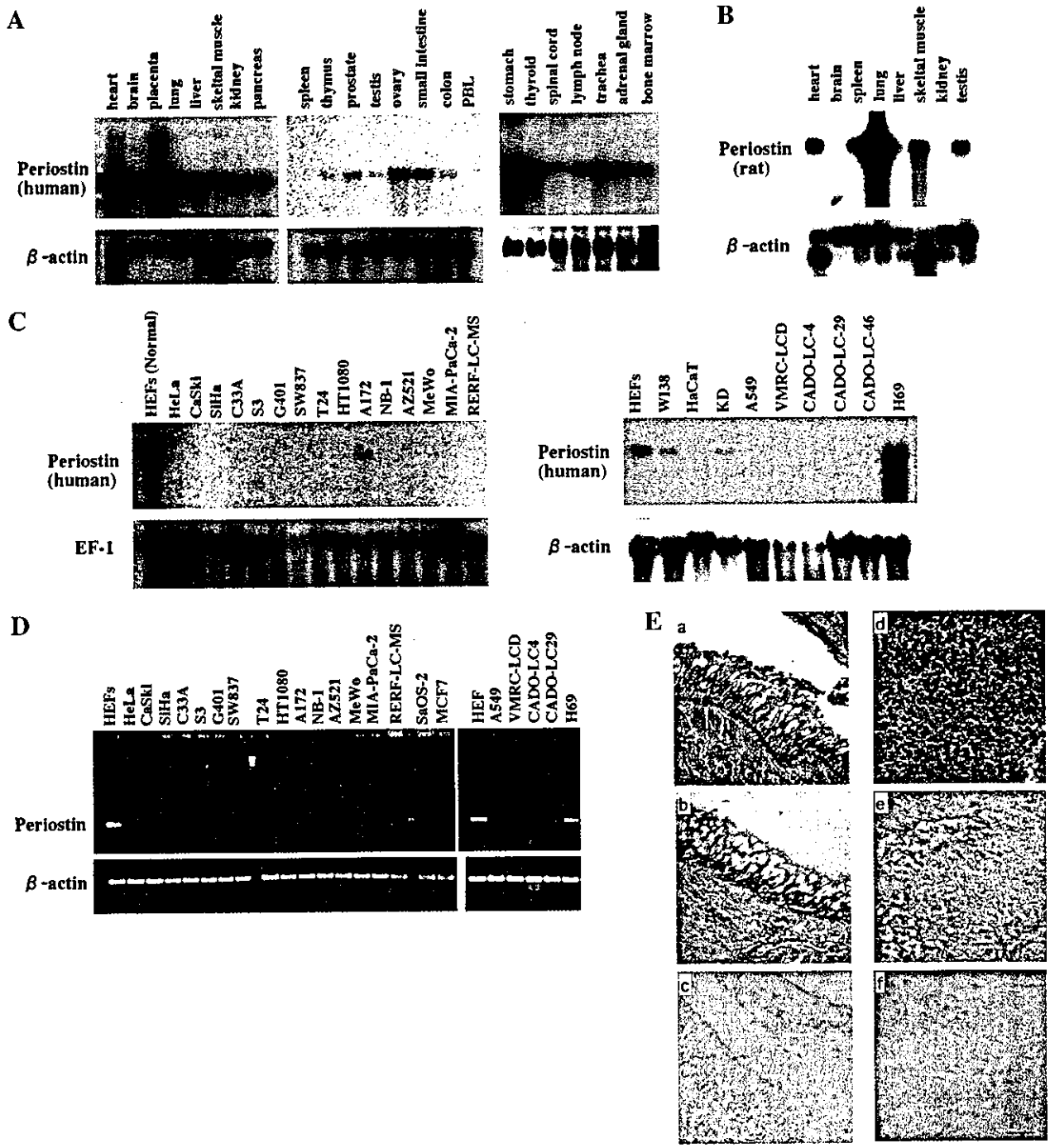

FIG. 1. Periostin mRNA expression in normal and tumor cell lines and tissues. Northern blot analysis of periostin expression in normal human (A) and rat (B) tissues and in human cancer cell lines (C—left: total RNA blot, right: poly(A) RNA blot) by use of human or rat periostin cDNA probes. HEF, human embryo fibroblasts; HeLa, CaSki, SiHa, C33A, cervical cancer; S3, endometrial cancer; G401, Wilms' tumor; SW837, colon cancer; T24, bladder cancer; HT1080, fibrosarcoma; A172, glioblastoma; NB-1, neuroblastoma; AZ521, gastric cancer; MeWo, melanoma; MIA-PaCa-2, pancreatic cancer; RERF-LC-MS, lung cancer; WI38, normal human fibroblasts; HaCaT, skin keratinocyte (immortalized); KD, human normal fibroblasts; A549, VMRC-LCD, CADO-LC4, CADO-LC29, CADO-LC46, H69, lung cancer; PBLs, peripheral blood leukocytes; EF-1, elongation factor 1. (D) RT-PCR analysis of periostin mRNA expression in normal cells and tumor lines. Most of the tumor cell lines mentioned in (C) were tested, as were the osteosarcoma line SaOS-2 and the breast cancer line MCF7. (E) Presence of periostin transcripts in lung cancer tissues. Lung cancer tissues (e, f) as well as a tissue from normal bronchial epithelium (b, c) were analyzed by *in situ* mRNA hybridization using digoxigenin-labeled sense (c, f) or antisense (b, e) periostin riboprobes. Sections stained with hematoxylin and eosin (H&E) are also shown (a, d). Bar = 30 μm.

mRNA is expressed in the lung and heart of mice has been previously revealed by dot-blot RNA hybridization and *in situ* RNA hybridization [2, 11]. Figure 1C indicates the expression of periostin mRNA in a variety of human normal and cancer cell lines and shows that periostin mRNA is detected in normal human cells such as HEFs, WI38, and KD but not in an immortalized skin keratinocyte cell line, HaCaT. Of the cancer cell lines, two—A172 (glioblastoma) and H69 (small cell lung cancer)—expressed periostin mRNA. In contrast, periostin mRNA was not detected in any of the remaining cancer cell lines, namely, cervical cancer cell lines HeLa, CaSki, SiHa, and C33A, endometrial cancer cell line S3, Wilms' tumor cell line G401, colon cancer cell line SW837, bladder cancer cell line T24, fibrosarcoma cell line HT1080, neuroblastoma cell line NB-1, gastric cancer cell line AZ521, melanoma cell line MeWo, pancreatic cancer cell line MIA-PaCa-2, and non-small cell lung cancer cell lines RERF-LC-MS, A549, VMRC-LCD, CADO-LC4, CADO-LC29, and CADO-LC46. To assess whether the tumor cell lines could express low levels of periostin mRNA, we used RT-PCR to detect periostin mRNA in the RNA samples of the above-mentioned tumor lines, as well as in RNA preparations of two additional tumor lines, osteosarcoma line SaOS-2 and breast cancer line MCF7. Periostin mRNA was not detected by RT-PCR in CaSki, SiHa, S3, SW837, T24, HT1080, NB-1, MeWo, MIA-PaCa-2, A549, VMRC-LCD, CADO-LC4, and CADO-LC29 cells, but it was found in HeLa, C33A, G401, A172, AZ521, and RERF-LC-MS cells, although the expression levels in the latter lines were significantly lower than that in normal cells (HEFs) (Fig. 1D). Periostin expression was also faintly detected in SaOS-2 cells but none was observed in MCF7 cells (Fig. 1D).

To determine whether periostin mRNA expression is also downregulated in human cancer tissues, we examined the expression of periostin mRNA in lung cancer tissues by *in situ* mRNA hybridization. The periostin transcript was detected in normal bronchial and alveolar epithelium by an antisense probe (Fig. 1Eb and data not shown), but its expression was suppressed in all three small cell lung carcinoma tissues (Fig. 1Ee and data not shown), two of three atypical carcinoid tumors, two of three typical carcinoid tumors, an alveolar carcinoma (well differentiated), and a well-differentiated adenocarcinoma (data not shown). Positive signals within the tumor sites in Fig. 1Ee are due to the infiltration of lymphocytes, which serve as an internal control of the assay. Positive signals in the tumor were detected in one poorly differentiated alveolar carcinoma, one of three atypical carcinoid tumors, and one of three typical carcinoid tumors (data not shown). When a sense probe was used as a negative control, no signals were detected (Figs. 1Ec, 1Ef, and data not shown). These observations reveal that periostin mRNA is downregulated in a variety of human cancer cell lines and several human lung cancers, indicating that downregulation of periostin mRNA expression generally correlates with the development of human cancers.

Periostin Suppresses the Anchorage-Independent Growth of Human Cancer Cell Lines

To assess whether additional periostin expression could suppress the transformed phenotypes of human cancer cell lines, we introduced the periostin gene into human cancer cell lines by infection with a retrovirus vector and examined the anchorage-independent growth of these cells, that is, colony formation in soft agar. To introduce the periostin gene into human cancer cell lines, we constructed an amphotropic retrovirus vector containing the rat periostin gene tagged with HA at its C terminus (pCXbsr/Peri). This virus and the control vector virus (pCXbsr) were introduced into the bladder carcinoma cell line T24 and the osteosarcoma cell line SaOS-2. In these cell lines, the expression of periostin mRNA is normally downregulated, although large deletions or rearrangements in this gene could not be detected by Southern blot analysis. Cancer cells infected with these viruses were selected with blasticidin S for 10 days, after which drug-resistant colonies were pooled and the colony formation of these cells in soft agar was assayed. As shown in Fig. 2A, the colony-forming ability of the cells expressing exogenous periostin was significantly lower than that of the parental cells with and without the control vector virus. However, the growth rate of the cells expressing periostin was similar to that of the control cells (Fig. 2C), indicating that proliferation of the cancer cells was not affected by this gene. That the periostin protein, which is tagged by HA, was indeed expressed in the pCXbsr/Peri-infected cells was confirmed by Western blotting with an anti-HA antibody (Fig. 2B). These observations indicate that periostin is able to suppress the anchorage-independent growth of malignant cancer cells.

Deletion of the C-Terminal Region of Periostin Abrogates Its Suppressor Activity

The translated cDNA sequence of the periostin protein indicates that it encodes a typical signal peptide sequence at its N-terminal end and bears four repeated domains (RDS), each containing two highly conserved sequences found in the fasciclin I family of proteins [3] (Fig. 3A). To identify the regions responsible for the suppressor activity of periostin, we constructed three deletion mutants of periostin that lack either the N-terminal region (ΔN), the C-terminal region (ΔC), or both terminal regions (ΔNC) (Fig. 3A). Recombinant amphotropic retroviruses containing these periostin

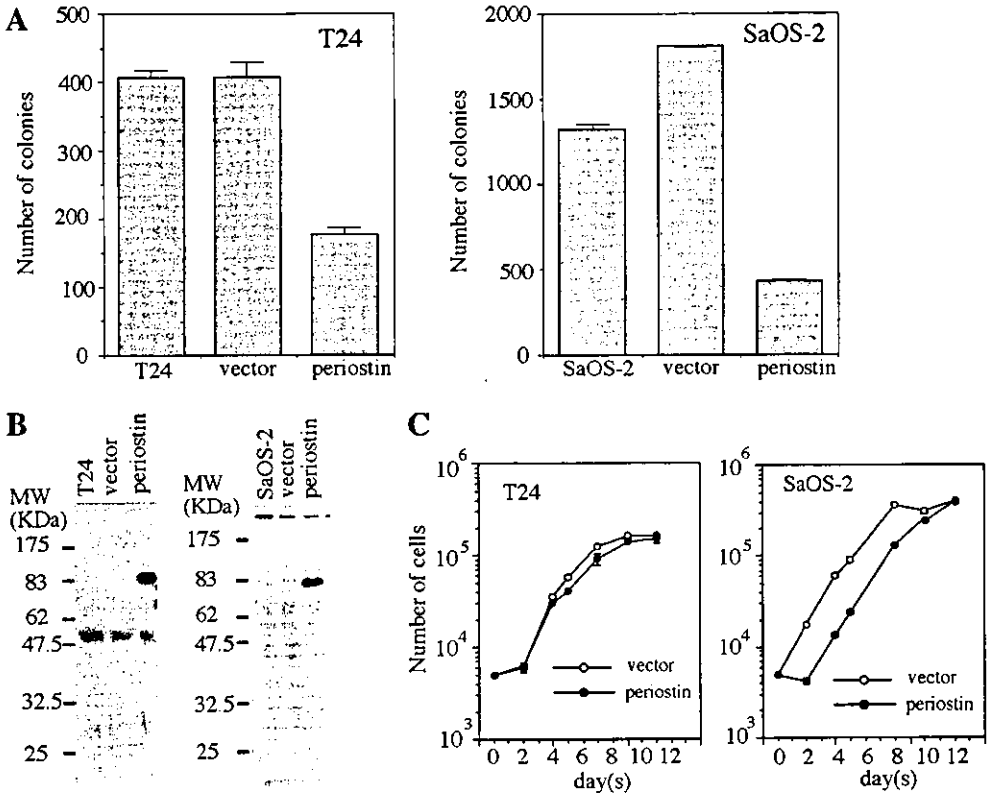

FIG. 2. Effect of periostin on the anchorage-independent growth of T24 and SaOS-2. (A) Colony formation in soft agar. T24 (bladder cancer) and SaOS-2 (osteosarcoma) were infected with the pCXbsr vector virus (vec) or recombinant virus containing HA-taggedperiostin. Blasticidin S-resistant cells were pooled and 10^4 cells were incubated into 0.4% soft agar. Colonies were scored after incubation for 3 weeks. The experiment was performed with duplicate samples. The number of colonies indicates the mean value obtained from duplicate samples, and the bar represents the standard deviation from the mean value. Similar results were obtained in five independent experiments. (B) Expression of HA-tagged periostin protein in T24 (left) and SaOS-2 (right) cells. Cell lysates from T24 cells were concentrated by immunoprecipitation with an anti-HA polyclonal antibody. Immunoprecipitated complexes or cell lysate was separated by SDS–PAGE and detected by Western blotting using a mouse HA-specific antibody (left) or a rat HA-specific antibody (right). (C) Growth curves of T24 and SaOS-2 cells. Five thousand cells were seeded in growth medium in 24-well culture plates. The growing cells in duplicate plates were trypsinized and counted.

mutants as well as wild-type (WT) periostin were introduced into the bladder carcinoma cell line T24. After blasticidin S selection, the colony-forming ability of these cells in soft agar was investigated. As shown in Figs. 3B (left) and 3D, the wild type and the ΔN mutant of periostin significantly suppressed colony formation in soft agar. However, the ΔC and ΔNC mutants failed to suppress colony formation in soft agar, indicating that the C-terminal region of periostin is required for the suppressor activity of this protein. To determine whether the C-terminal region is enough to suppress anchorage-independent growth, we examined the suppressor activity of a mutant periostin containing only the C-terminal region (C-term). As shown in Fig. 3B (right), expression of C-term periostin suppressed the colony formation of T24 cells in soft agar. Suppression of anchorage-independent growth by the C-term virus was also observed in SaOS-2 cells (data not shown). That the WT and mutant periostin proteins were expressed was confirmed by Western blotting with the anti-HA antibody (Fig. 3C). These observations indicate that the C-terminal region of periostin is sufficient to suppress the anchorage-independent growth of cancer cells.

Tumor Suppressor Function of Periostin Is Implemented by an Unsecreted Pool of Periostin

Periostin protein has a typical signal peptide sequence at its N-terminal region and is normally secreted into the culture medium [3]. Our experiments with the periostin deletion mutants indicated that the periostin mutants lacking the signal peptide sequence (ΔN and C-term) were still able to suppress anchorage-independent tumor cell growth, indicating that intracellular periostin may be responsible for this suppression. To clarify whether these periostin mutants are secreted into the culture medium, we transfected all

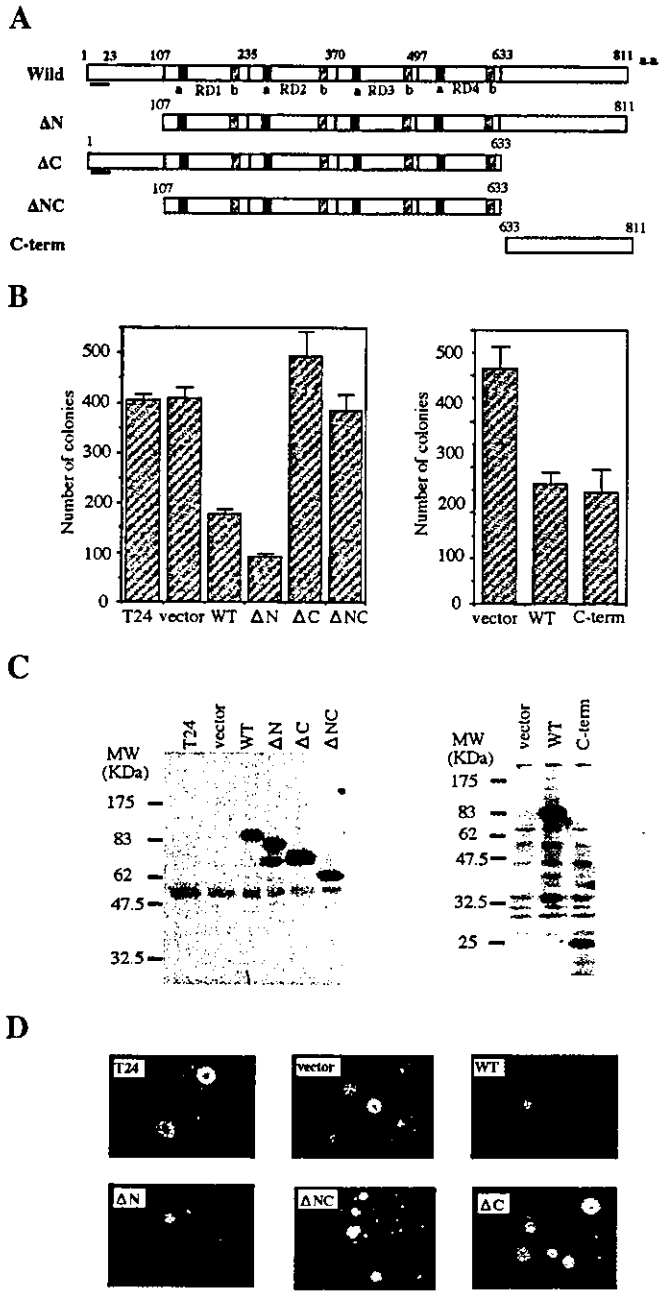

FIG. 3. Effects of deletions in periostin on its ability to suppress the anchorage-independent growth of T24. (A) Structure of periostin and four deletion mutants (ΔN, ΔC, ΔNC, and C-term). The bar at the N terminus represents the position of the typical signal peptide sequence. The HA tag is attached to the C terminus of each construct. Repeated domains (RDs) each contain two highly conserved sequences that are indicated by black boxes (a) and hatched boxes (b). (B) Colony formation in soft agar of T24 cells infected with the pCXbsr vector virus (vec) or the recombinant viruses containing wild-type periostin (WT) or its mutants (ΔN, ΔC, ΔNC, C-term). Colonies were scored after incubation for 3 weeks. The experiment was performed with duplicate samples. The number of colonies is the mean value obtained from duplicate samples, and the bar represents the standard deviation from the mean value. Similar results were obtained in three independent experiments. (C) Expression of wild-type and mutant periostin proteins in infected T24 cells. Immunoprecipitation and Western blotting were carried out as described in the legend to Fig. 2 and Materials and Methods. (D) Suppression of anchorage-independent growth in T24 cells by periostin. Colonies in soft agar were photographed.

the periostin mutants into a human kidney cell line, 293T cells, and collected and concentrated the culture medium (see Fig. 4 legend). The presence of periostin protein was measured by Western blotting. As shown in Fig. 4A (left), wild-type and ΔC periostin proteins, both of which contain the signal peptide sequence, were detected in the culture medium, while ΔN and ΔNC mutant proteins, which lack the signal peptide sequences, were not. However, all periostin proteins were detected in each cell lysate (Fig. 4A, right). These observations indicate that the periostin mutants lacking the signal peptide sequence are not secreted into the culture medium and remain in cells, and thus must exert their tumor suppressor activity within the cell. This is supported by fluorescence microscopy experiments investigating the subcellular localization of wild-type or C-term periostin fused with GFP. As shown in Fig. 4B, GFP signals of wild and C-term periostin proteins were detected in both cytoplasm and nucleus of the transfected cells. Western blotting confirmed that these transfected cells expressed the GFP-linked periostin protein (Fig. 4C). These observations show that periostin not only is secreted into culture medium but also remains in cytoplasm and nucleus, suggesting that the nonsecreted periostin pool is involved in suppressing anchorage-independent growth.

DISCUSSION

In this study, we initially demonstrated that periostin mRNA is generally downregulated in a variety of human cancer cell lines and human lung cancer tissues. Furthermore, we showed that periostin is able to suppress the anchorage-independent growth of cancer cell lines such as T24 and SaOS-2. These observations suggest that periostin may act as a tumor suppressor to inhibit human oncogenesis. It may be that the downregulation of periostin in tumor cells is due to damage to the periostin gene, as the human genome database shows that the human periostin gene is located next to the transient receptor potential channel 4 gene, which maps to the chromosome 13q13 region [12], and chromosomal alterations around this region have been observed in several human cancers [13, 14, 17]. Supporting this notion are preliminary Southern blot analyses of human lung cancer cell lines, including A549, CADO-LC4, CADO-LC29, CADO-LC46, and H69, which revealed two types of restriction fragment length polymorphisms (RFLPs) in the periostin gene (data not shown). However, further analysis is re-

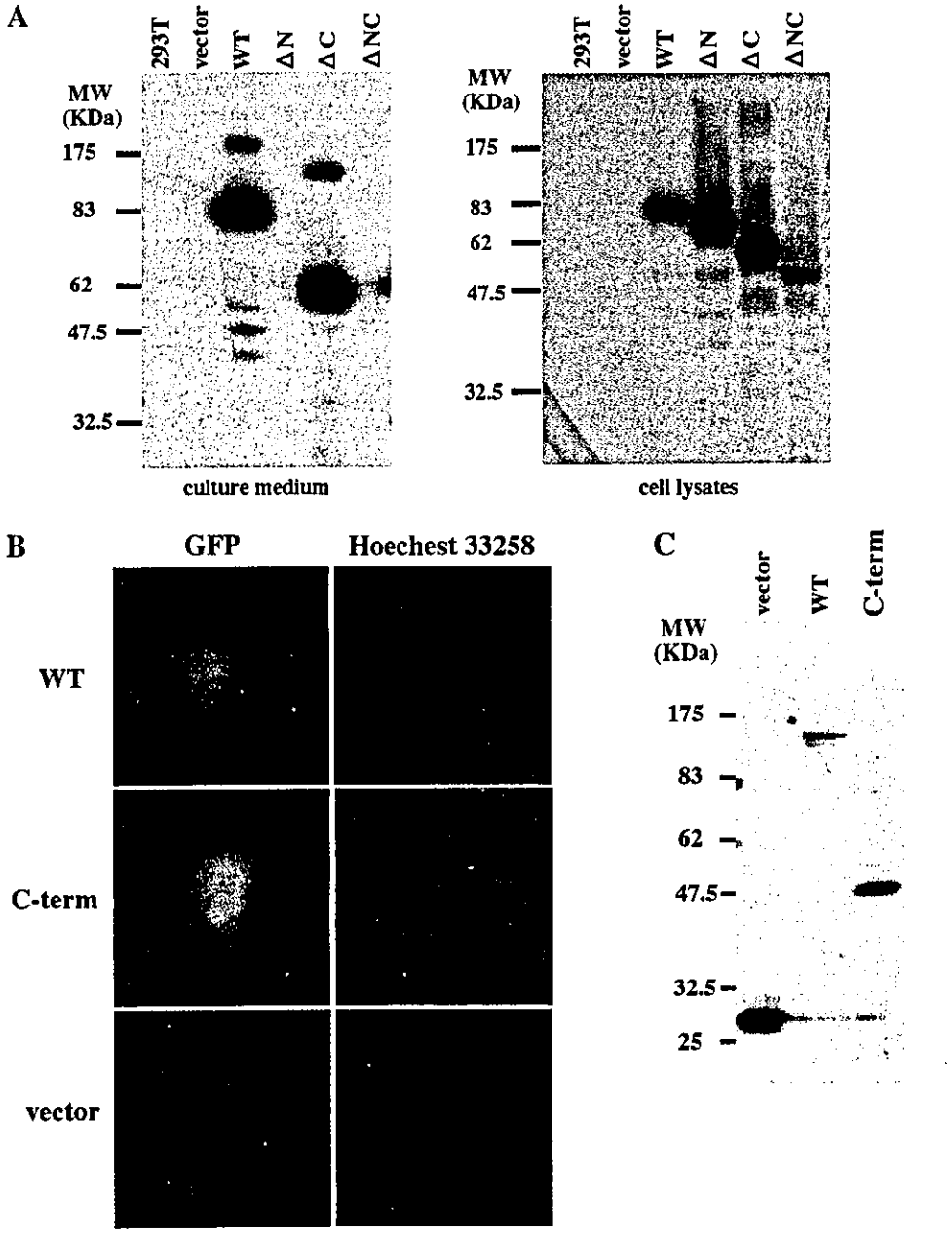

FIG. 4. Subcellular localization of periostin. (A) Effects of deletions in periostin on its secretion from the cell. 293T cells were transfected with the pCXbsr vector (vec) or pCXbsr containing HA-tagged periostin (WT, ΔN, ΔC, and ΔNC). The conditioned medium and cell lysate of transfected cells were collected after incubation for 2 days. The conditioned medium was concentrated 30-fold using a centrifugal filter device (UFV5BGC25, MILLIPORE). HA-tagged periostin protein was detected by Western blotting using an anti-HA antibody (3F10). (B) Subcellular localization of periostin. COS7 cells, a monkey kidney cell line, were transfected with the pcDNA3 vector containing GFP or periostin (WT and C-term) fused with GFP at its C terminus. The cells were fixed with 4% paraformaldehyde 48 h after transfection and photographed under a fluorescence microscope. (C) Western blotting of GFP and GFP-fused periostin in transfected COS7 cells using anti-GFP antibody.

quired to show whether the presence of the RFLPs indeed correlates negatively with the expression of periostin mRNA. Another possible explanation of the downregulation of periostin mRNA in tumor cells is that transcriptional regulation of the periostin gene is disturbed. It has been reported that periostin protein expression is increased by stimulation with TGF-β in primary osteoblast cells [3] or with bone morphogenetic protein 2 (BMP-2) in mesenchymal cells [15]. Furthermore, periostin protein expression can be downregulated by introducing Wnt-3 or by inhibiting GSK-3β [8]. Thus, the downregulation of periostin expression in

cancer cell lines or tissues could be caused by activation of WNT signal transduction or by inhibition of TGF-β signal transduction. Determining how periostin expression is regulated will aid our understanding of how this gene participates in suppressing oncogenesis.

We showed that the C-terminal region of periostin is sufficient for the suppression of anchorage-independent growth of tumor cell lines. The periostin protein bears a typical N-terminal signal peptide sequence and four repeated domains containing sequences that are conserved in the fasciclin I family of proteins, which include βig-h3 and fasciclin I [2, 3]. The fasciclin I protein family is found in a wide range of species, including mammals, insects, sea urchins, plants, yeast, and bacteria [16], and several reports have suggested that these proteins, including periostin, act as adhesion molecules [3, 5, 6, 16]. This suggests that the conserved sequences in the periostin repeats may play a role in cell adhesion. However, the C-terminal region of periostin, which is solely responsible for the ability of the protein to suppress anchorage-independent growth, is not conserved in the fasciclin I protein family. Furthermore, the C-terminal region exhibits no significant amino acid homology with database proteins. We found that deletion mutants of periostin that lacked the signal peptide sequence were not secreted into the culture medium but nevertheless were suppressive of the anchorage-independent growth of cancer cells, indicating that an intracellular periostin pool is critical for this suppressor function. Moreover, GFP-fused periostin protein was also detected in the cytoplasm and nucleus of transfected cells as well as in the culture medium, suggesting that only part of the periostin pool is secreted normally. This supports the notion that periostin has a dual function, one as a secreted cell adhesion molecule, a function that is conserved in the fasciclin I protein family, and another as a cytoplasmic and nuclear regulator of anchorage-independent growth. Further experiments are necessary to clarify the mechanisms by which periostin mRNA expression is downregulated in cancer cells and by which periostin suppresses anchorage-independent tumor growth. These studies would provide new insights into dysregulated growth controls that lead to human carcinogenesis.

We are grateful to Dr. T. Kijima for providing the CADO-LC4, CADO-LC29, CADO-LC46, VMRC-LCD, A549, and H69 cell lines and to the Japanese Collection of Research Bioresources (JCRB) for the HeLa, G401, SW837, HT1080, A172, NB-1, AZ521, MeWo, MIA-PaCa-2, RERF-LC-MS, and WI38 cell lines. We also thank Dr. T. Akagi for the pCXbsr vector.

This work was supported by a Grant-in-Aid for the Encouragement of Young Scientists, Japan Society for the Promotion of Science, a grant-in-aid from the Osaka Cancer Foundation, and a grant-in-aid from the Charitable Trust Osaka Cancer Researcher Fund.

REFERENCES

1. Yoshioka, N., Inoue, H., Nakanishi, K., Oka, K., Yutsudo, M., Yamashita, A., Hakura, A., and Nojima, H. (2000). Isolation of transformation suppressor genes by cDNA subtraction: Lumican suppresses transformation induced by v-src and v-K-ras. *J. Virol.* **74,** 1008–1013.
2. Takeshita, S., Kikuno, R., Tezuka, K., and Amann, E. (1993). Osteoblast-specific factor 2: Cloning of a putative bone adhesion protein with homology with the insect protein fasciclin I. *Biochem. J.* **294,** 271–278.
3. Horiuchi, K., Amizuka, N., Takeshita, S., Takamatsu, H., Katsuura, M., Ozawa, H., Toyama, Y., Bonewald, L. F., and Kudo, A. (1999). Identification and characterization of a novel protein, periostin, with restricted expression to periosteum and periodontal ligament and increased expression by transforming growth factor β. *J. Bone Miner. Res.* **14,** 1239–1249.
4. Skonier, J., Neubauer, M., Madisen, L., Bennett, K., Plowman, G. D., and Purchio, A. F. (1992). cDNA cloning and sequence analysis of βig-h3, a novel gene induced in a human adenocarcinoma cell line after treatment with transforming growth factor-β. *DNA Cell Biol.* **11,** 511–522.
5. LeBaron, R. G., Bezverkov, K. I., Zimber, M. P., Pavelec, R., Skonier, J., and Purchio, A. F. (1995). βIG-H3, a novel secretory protein inducible by transforming growth factor-β, is present in normal skin and promotes the adhesion and spreading of dermal fibroblasts in vitro. *J. Invest. Dermatol.* **104,** 844–849.
6. Ohno, S., Noshiro, M., Makihira, S., Kawamoto, T., Shen, M., Yan, W., Kawashima-Ohya, Y., Fujimoto, K., Tanne, K., and Kato, Y. (1999). RGD-CAP (βig-h3) enhances the spreading of chondrocytes and fibroblasts via integrin $\alpha1\beta1$. *Biochim. Biophys. Acta* **1451,** 196–205.
7. Skonier, J., Bennett, K., Rothwell, V., Kosowski, S., Plowman, G., Wallace, P., Edelhoff, S., Disteche, C., Neubauer, M., Marquardt, H., *et al.* (1994). βig-h3: A transforming growth factor-β-responsive gene encoding a secreted protein that inhibits cell attachment in vitro and suppresses the growth of CHO cells in nude mice. *DNA Cell Biol.* **13,** 571–584.
8. Haertel-Wiesmann, M., Liang, Y., Fantl, W. J., and Williams, L. T. (2000). Regulation of cyclooxygenase-2 and periostin by Wnt-3 in mouse mammary epithelial cells. *J. Biol. Chem.* **275,** 32046–32051.
9. Akagi, T., Shishido, T., Murata, K., and Hanafusa, H. (2000). v-Crk activates the phosphoinositide 3-kinase/AKT pathway in transformation. *Proc. Natl. Acad. Sci. USA* **97,** 7290–7295.
10. Shimakage, M., and Sasagawa, T. (2001). Detection of Epstein–Barr virus-determined nuclear antigen-2 mRNA by in situ hybridization. *J. Virol. Methods* **93,** 23–32.
11. Kruzynska-Frejtag, A., Machnicki, M., Rogers, R., Markwald, R. R., and Conway, S. J. (2001). Periostin (an osteoblast-specific factor) is expressed within the embryonic mouse heart during valve formation. *Mech. Dev.* **103,** 183–188.
12. McKay, R. R., Szymeczek-Seay, C. L., Lievremont, J. P., Bird, G. S., Zitt, C., Jungling, E., Luckhoff, A., and Putney, J. W., Jr. (2000). Cloning and expression of the human transient receptor potential 4 (TRP4) gene: Localization and functional expression of human TRP4 and TRP3. *Biochem. J.* **351,** 735–746.
13. La Starza, R., Wlodarska, I., Aventin, A., Falzetti, D., Crescenzi, B., Martelli, M. F., Van den Berghe, H., and Mecucci, C. (1998). Molecular delineation of 13q deletion boundaries in 20 patients with myeloid malignancies. *Blood* **91,** 231–237.

14. De Rienzo, A., Jhanwar, S. C., and Testa, J. R. (2000). Loss of heterozygosity analysis of 13q and 14q in human malignant mesothelioma. *Genes Chromosomes Cancer* **28,** 337–341.
15. Ji, X., Chen, D., Xu, C., Harris, S. E., Mundy, G. R., and Yoneda, T. (2000). Patterns of gene expression associated with BMP-2-induced osteoblast and adipocyte differentiation of mesenchymal progenitor cell 3T3-F442A. *J. Bone Miner. Metab.* **18,** 132–139.
16. Kawamoto, T., Noshiro, M., Shen, M., Nakamasu, K., Hashimoto, K., Kawashima-Ohya, Y., Gotoh, O., and Kato, Y. (1998). Structural and phylogenetic analyses of RGD-CAP/βig-h3, a fasciclin-like adhesion protein expressed in chick chondrocytes. *Biochim. Biophys. Acta.* **1395,** 288–292.
17. Stokke, T., DeAngelis, P., Smedshammer, L., Galteland, E., Steen, H. B., Smeland, E. B., Delabie, J., and Holte, A. H. H. (2001). Loss of chromosome 11q21-23.1 and 17p and gain of chromosome 6p are independent prognostic indicators in B-cell non-Hodgkin's lymphoma. *Br. J. Cancer* **85,** 1900–1913.

Received March 19, 2002
Revised version received June 7, 2002

The EMBO Journal Vol. 21 No. 11 pp. 2807–2818, 2002

The meiotic recombination checkpoint is regulated by checkpoint *rad*$^+$ genes in fission yeast

Midori Shimada, Kentaro Nabeshima, Takahiro Tougan and Hiroshi Nojima[1]

Department of Molecular Genetics, Research Institute for Microbial Diseases, Osaka University, 3-1 Yamadaoka, Suita City, Osaka 565-0871, Japan

[1]Corresponding author
e-mail: hnojima@biken.osaka-u.ac.jp

During the course of meiotic prophase, intrinsic double-strand breaks (DSBs) must be repaired before the cell can engage in meiotic nuclear division. Here we investigate the mechanism that controls the meiotic progression in *Schizosaccharomyces pombe* that have accumulated excess meiotic DSBs. A meiotic recombination-defective mutant, *meu13Δ*, shows a delay in meiotic progression. This delay is dependent on *rec12*$^+$, namely on DSB formation. Pulsed-field gel electrophoresis analysis revealed that meiotic DSB repair in *meu13Δ* was retarded. We also found that the delay in entering nuclear division was dependent on the checkpoint *rad*$^+$, *cds1*$^+$ and *mek1*$^+$ (the meiotic paralog of Cds1/Chk2). This implies that these genes are involved in a checkpoint that provides time to repair DSBs. Consistently, the induction of an excess of extrinsic DSBs by ionizing radiation delayed meiotic progression in a *rad17*$^+$-dependent manner. *dmc1Δ* also shows meiotic delay, however, this delay is independent of *rec12*$^+$ and checkpoint *rad*$^+$. We propose that checkpoint monitoring of the status of meiotic DSB repair exists in fission yeast and that defects other than DSB accumulation can cause delays in meiotic progression.

Keywords: DNA damage checkpoint/double-strand break/homologous recombination/meiosis/pachytene checkpoint

Introduction

Meiosis is a special type of cell division that produces haploid gametes from diploid parental cells. During meiosis, homologous recombination occurs at a high frequency and can generate new allelic combinations in the resulting gametes, thereby increasing the genetic diversity of the offspring and promoting the survival of the species during critical environmental changes. Homologous recombination is also essential for ensuring that chromosome segregation occurs correctly during meiosis. In the absence of recombination, homologs mis-segregate and the resulting anneuploid gametes produce defective or inviable progeny. Thus, homologous recombination is vital for the generation of viable gametes (Kleckner, 1996; Roeder, 1997).

When there are defects in critical cell cycle events, checkpoint mechanisms delay the cell cycle progression so as to prevent aneuploidy and cell lethality (Hartwell and Weinert, 1989). This arrest or delay in cell cycle progression occurs in eukaryotic cells when they are exposed to DNA-damaging agents or when DNA synthesis is blocked. The checkpoints require the function of the checkpoint *rad*$^+$ genes (*rad1*$^+$, *rad3*$^+$, *rad9*$^+$, *rad17*$^+$, *rad26*$^+$ and *hus1*$^+$), *crb2*$^+$/*rhp9*$^+$, *cds1*$^+$ and *chk1*$^+$ (Caspari and Carr, 1999) and also inhibit Tyr15 dephosphorylation of Cdc2 (Rhind *et al.*, 1997; Rhind and Russell, 1998). It has been found that a pre-meiotic replication checkpoint also operates in both budding and fission yeasts (Stuart and Wittenberg, 1998; Murakami and Nurse, 1999).

There are several meiotic mutants such as *hop2Δ* (*Saccharomyces cerevisiae* homolog of *meu13*), *dmc1Δ* and *zip1Δ* that exhibit an arrest at the pachytene stage of meiotic prophase in *S.cerevisiae* (Roeder and Bailis, 2000). Mammalian germ cells exhibit meiotic arrest and apoptosis in response to the defects of recombination and/or synapsis, suggesting the conservation throughout evolution of a checkpoint that prevents entry into meiosis I (Roeder and Bailis, 2000). Thus, to ensure the generation of viable meiotic products, the progression through meiosis must be tightly regulated by mechanisms that monitor the status of recombination repair, synaptonemal complex (SC) formation and proper chromosome segregation.

In *S.cerevisiae*, several proteins (Mec1, Rad24 and Rad17) involved in the DNA damage checkpoint also participate in the pachytene checkpoint (Lydall *et al.*, 1996). In mammals, Atm, Atr, Rad1 and Chk1 proteins, which are involved in the damage checkpoint, also localize to the meiotic chromosomal cores and are thought to play important roles in meiotic recombination, meiotic arrest and apoptosis (Roeder and Bailis, 2000). In *S.cerevisiae* and probably also in mammals, all mutants that arrest at the pachytene stage exhibit defects in SC formation as well as in recombination. For this reason, it is not yet clear whether the defects in recombination or synapsis are responsible for the arrest in cell cycle progression that is mediated by the pachytene checkpoint. As *Schizosaccharomyces pombe* does not form an SC, meiotic recombination in *S.pombe* is a good model for studying the meiotic checkpoint during prophase.

In fission yeast, no meiotic recombination-deficient mutants show meiotic arrest and the precise meiotic progression in meiotic recombination-deficient mutants has not been fully investigated so far. To examine these aspects, we previously isolated and analyzed *meu13*$^+$ (Nabeshima *et al.*, 2001), a homolog to budding yeast *HOP2*, and *dmc1*$^+$ (Fukushima *et al.*, 2000), a meiotic RecA homolog that is conserved among a variety of organisms. Here, we report that *meu13Δ* cells show a delay in entering into meiosis I. The checkpoint Rad proteins (Rad17, Rad3, Rad1 and Rad9), Cds1 and the meiotic-